Upper critical fields of regular superconductive networks. Surfaces and impurities

J. M. Simonin, C. Wiecko, and A. López
Centro Atómico Bariloche, Comisión Nacional de Energía Atómica and Instituto Balseiro, Comisión Nacional de Energía Atómica and Universidad Nacional de Cuyo, 8400 Bariloche, Argentina
(Received 3 December 1982)

The upper critical field of several defect structures is studied using the de Gennes–Alexander theory of superconductive networks. The systems considered include a terminated ladder, an impurity site within the ladder, and a square lattice with a surface. Localized modes of condensation appear in all the structures considered. Four different methods have been used alternatively or concurrently: direct diagonalization, continuous-fraction expansion, transfer matrix, and a renormalization-group decimation procedure. This last method has proved very useful to study irrational values of the ratio flux to flux quantum in the square lattice. The case of the square lattice with a surface shows several characteristics in common with surface superconductivity (H_{c3}) in bulk materials.

I. INTRODUCTION

The de Gennes–Alexander theory[1] of superconductive networks, first envisaged as a theory of inhomogeneous superconductors, yields, as was shown in a previous paper, quite interesting results when applied to regular superconductive networks.[2] Based on solutions of the linearized Ginzburg-Landau equations, the theory gives the magnetic phase boundary of nets of thin wires which behave as weak links, joining the nodes.[3]

In Ref. 2 we had studied an infinite ladder, for which we found a critical value ϕ_1 of the flux per square ϕ, such that for $\phi<\phi_1$ superconductivity condenses in a uniform mode and for $\phi>\phi_1$ a modulated structure appears. In this paper we want to discuss some applications to defects in an otherwise regular array, a necessary step to understand the behavior of real systems whose experimental realization may not be too far ahead.[4] In Sec. II of this paper we discuss the transfer matrix[5] and a renormalization-group decimation[6] (RGD) applied to the infinite ladder and then we use both methods to deal with a semi-infinite ladder. We find that superconductivity nucleates at higher temperatures in the defect structure, giving rise to a localized mode. The methods are complementary because the RGD is very effective in giving the phase boundary, whereas the transfer matrix is more adequate for the discussion of the spatial variation of the order parameter. At the end of Sec. II we have used the transfer matrix to discuss the properties of an impurity in the ladder, i.e., the case when one loop in the infinite ladder is of different size from the rest. We find that a localized mode nucleates around the impurity at a temperature higher than required for the whole structure to become superconducting.

In Sec. III we study the two-dimensional (2D) square lattice with a border or surface. As in the previous cases here again the defect nucleates a localized mode at temperatures higher than the transition temperature for the perfect structure. The properties of the surface mode resemble very much those of surface superconductivity in a bulk material. For the sake of comparison we have, in that section, also studied the infinite square lattice, obtaining the phase boundary by use of fractional values of ϕ/ϕ_0 ($\phi_0=e/hc$) and diagonalizing the implied basis.[7] As alternative techniques we have decimated the nodes within the basis and finally also applied the RGD directly to the original equations. This method can be used to discuss irrational values of the ratio flux per square to flux quantum, which cannot be treated by any of the other procedures. We have checked the statement[8] by Aubry, according to which the superconducting square lattice would be a special case of a more general electronic problem which can have both localized and extended states. The superconducting case lies on the critical values of the parameters where the crossover occurs.

As noted in Ref. 2, when studying structures with a border the first eigenvalue is always associated with surface properties. At the end of Sec. III we have discussed the case of a multiple ladder and shown how the first and second eigenvalues give phase diagrams and order parameters resembling

surface and "bulk" modes, respectively. This is similar to the case of the Ginzburg-Landau (GL) differential equation, which gives H_{c2} and H_{c3}, depending on the boundary conditions.

II. TERMINATED LADDER AND IMPURITY

A. Infinite ladder and surface

In Ref. 2 we considered 2D lattices built from N equally spaced infinite wires joined by transverse strands. The structure obtained for $N=2$ we called the "ladder," for which the nodal equations in matrix form read

$$\underline{H}_0\underline{\psi}_n+\underline{U}\underline{\psi}_{n-1}+\underline{U}^\dagger\underline{\psi}_{n+1}=0\ , \tag{1}$$

where

$$\underline{\psi}=\begin{bmatrix}\psi_n^\uparrow\\ \psi_n^\downarrow\end{bmatrix}$$

is the order parameter in the upper and lower branches, and

$$\underline{H}_0=\begin{bmatrix}-3\cos l & 1\\ 1 & -3\cos l\end{bmatrix}\ ,\qquad U=\begin{bmatrix}e^{i\gamma} & 0\\ 0 & e^{-i\gamma}\end{bmatrix}\ . \tag{2}$$

Here l is the length of each branch normalized by the GL coherence length, $\gamma=\pi\phi/\phi_0$ with ϕ the flux per square.

To define the transfer matrix for this problem we introduce the infinite matrix $\underline{\mathscr{H}}$ made up of 2×2 blocks according to

$$\underline{\mathscr{H}}=\delta_{nn'}\underline{H}_0+\delta_{n,n'+1}\underline{U}+\delta_{n+1,n'}\underline{U}^\dagger\ ,$$

and define the resolvent matrix by the relation $\underline{G}(z)=(\underline{\mathscr{H}}-z\underline{\mathbb{1}})^{-1}$. The matrix elements of this resolvent satisfy

$$(\underline{H}_0-z\underline{\mathbb{1}})\underline{G}_{00}+\underline{U}^\dagger\underline{G}_{1,0}+\underline{U}\,\underline{G}_{-1,0}=\underline{\mathbb{1}}\ , \tag{3a}$$

$$(\underline{H}_0-z\underline{\mathbb{1}})\underline{G}_{n,0}+\underline{U}^\dagger\underline{G}_{n+1,0}+\underline{U}\,\underline{G}_{n-1,0}=\underline{0}\ \text{ for }\ n\neq0\ . \tag{3b}$$

Here the site $n=0$ is any arbitrarily chosen reference site on the ladder. We see from (1) and (3) that it is the pole of $\underline{G}$ at $z=0$ that determines the superconducting properties. We define left and right transfer matrices by the relations[5]

$$\underline{G}_{-n-1,0}=\underline{T}_L\underline{G}_{-n,0}\ ,\quad \underline{G}_{n+1,0}=\underline{T}_R\underline{G}_{n,0}\ . \tag{4}$$

Substituting Eq. (4) into (3), one obtains the relations

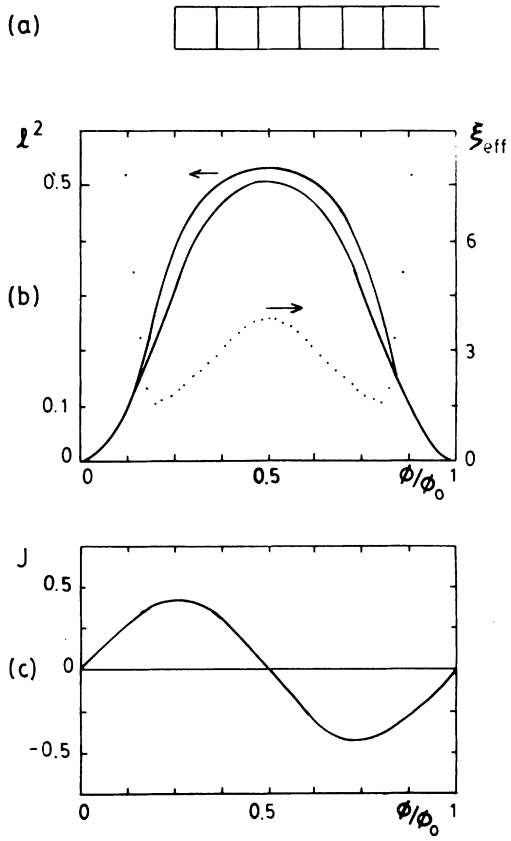

FIG. 1. Terminated ladder: (a) geometry; (b) phase diagram of the terminated ladder (lower solid line) compared with the one of the infinite ladder (upper solid line). Note that it is periodic in ϕ/ϕ_0. Also shown is the effective coherence length (dotted line), in units of L. (c) Current in the terminal branch, arbitrary units.

$$(\underline{H}_0+\underline{U}^\dagger\underline{T}_R+\underline{U}\,\underline{T}_L)\underline{G}_{00}=\underline{\mathbb{1}}\ ,$$
$$(\underline{H}_0+\underline{U}^\dagger\underline{T}_R+\underline{U}\,\underline{T}_R^{-1})=\underline{0}\ , \tag{5}$$
$$(\underline{H}_0+\underline{U}\,\underline{T}_L+\underline{U}^\dagger\underline{T}_L^{-1})=\underline{0}\ .$$

The problem of finding the phase diagram reduces now to finding the poles of $\underline{G}_{00}$, i.e., the zeros of the factor multiplying $\underline{G}_{00}$, in (5). The associated order parameter at site n can be determined through the transfer matrix by

$$\underline{\psi}_n=\underline{T}_R^n\underline{\psi}_0\ ,\quad \underline{\psi}_{-n}=\underline{T}_L^n\underline{\psi}_0\ ,\quad n\geq0\ , \tag{6}$$

where $\underline{\psi}_0$ is the eigenvector of $\underline{G}_{00}$ associated with the pole. It is easily verified that the above relations are completely equivalent to those obtained in Ref. 2, exploiting the translational invariance of the system. Equations (3)–(6) are more general because with due care they can be easily applied to cases where there is no translational invariance as for a surface or impurity.

For a semi-infinite ladder, Fig. 1(a), and assuming

that the surface is at $n=0$, Eq. (3a) changes to

$$\underline{H}_s\underline{G}_{00}+\underline{U}^{\dagger}\underline{G}_{10}=\underline{\mathbb{1}}\ , \tag{7}$$

where

$$\underline{H}_s=\begin{bmatrix}-2\cos l & 1\\ 1 & -2\cos l\end{bmatrix},$$

while the other equations remain unchanged. The transfer matrix allows us to obtain the relation

$$(\underline{H}_s+\underline{U}^{\dagger}\underline{T}_R)\underline{G}_{00}^{(s)}=\underline{\mathbb{1}}\ . \tag{8}$$

The poles of $\underline{G}_{00}^{(s)}$ determine the surface phase diagram. Figure 1(b) shows it together with the bulk phase boundary. The eigenvalues of the transfer matrix have a modulus less than 1 for l and γ on the surface phase boundary. This means that the surface will nucleate a localized mode whose amplitude decays exponentially as one moves away from the end point. Also shown in Fig. 1(b) is the effective coherence length, defined as $\xi_{\text{eff}}=1/\ln t$, where t is the modulus of the largest eigenvalue of T_R. Figure 1(c) shows the current in the first transverse branch which, as for the infinite ladder in Ref. 2, vanishes for $\phi/\phi_0=\frac{1}{2}$. It is seen from Fig. 1(b) that this fact is associated with an increase in the effective length ξ_{eff} since superconductivity is favored by the currentless branches which appear as a consequence of fluxoid quantization. This situation reflects itself also on the phase boundary which in this region moves closer to the bulk transition line.

Recently Sokoloff and José have devised a RGD technique[6] to deal with one-dimensional (1D) tight-binding problems. We have applied this method to some of the superconductive networks to obtain the phase boundary. The idea of Ref. 6 is to eliminate, from the set of equations defining a given tight-binding problem, the amplitude at every second node at each iteration. Thus, after r iterations, the procedure gives a new set of equations containing renormalized coefficients and showing couplings between sites which, in the original lattice, were a distance $2r$ apart. The power of the method lies in the fact that, in general, the coefficients connecting "nearest neighbors" in the renormalized lattice tend to zero quite rapidly (for most cases after 5–6 iterations), whereas the on-site coefficients have properties which allow one to determine the phase boundary from their behavior. For the ladder this implies that the phase diagram can be determined by a 2×2 on-site problem, in spite of the fact that, as solving the problem by other methods[2] show, the states are extended.

To illustrate the method let us go back to Eq. (1) and write it in the form

$$\underline{H}^{(0)}\underline{\psi}_n+\underline{U}^{(0)}\underline{\psi}_{n-1}+\underline{U}^{(0)\dagger}\underline{\psi}_{n+1}=0\ . \tag{1'}$$

We now eliminate from this set of equations every second node, counting from a given n. After repeating this procedure r times, we find

$$\underline{H}^{(r)}\underline{\psi}_n+\underline{U}^{(r)}\underline{\psi}_{n-2r}+\underline{U}^{(r)\dagger}\underline{\psi}_{n+2r}=0\ , \tag{9}$$

where

$$\underline{H}^{(r)}=\underline{H}^{(r-1)}-\underline{U}^{(r-1)}[\underline{H}^{(r-1)}]^{-1}\underline{U}^{(r-1)}-\underline{U}^{(r-1)\dagger}[\underline{H}^{(r-1)}]^{-1}\underline{U}^{(r-1)\dagger}\ ,$$

$$\underline{U}^{(r)}=-\underline{U}^{(r-1)}[\underline{H}^{(r-1)}]^{-1}\underline{U}^{(r-1)\dagger}\ . \tag{10}$$

Writing the matrices in the form

$$\underline{H}_0=\begin{bmatrix}a & b\\ b & a\end{bmatrix},\quad \underline{U}=\begin{bmatrix}c & d\\ d & c^*\end{bmatrix}, \tag{11}$$

we see that Eqs. (9) and (10) imply

$$\begin{aligned}
a_{(r)}&=a^{(r-1)}+\left[\frac{-2\,|c\,|^2a+4bd\,\mathrm{Re}c-2d^2a}{a^2-b^2}\right]_{(r-1)},\\
b^{(r)}&=b^{(r-1)}+\left[\frac{2d^2b+2b\,\mathrm{Re}c^2-4ad\,\mathrm{Re}c}{a^2-b^2}\right]_{(r-1)},\\
c^{(r)}&=\left[\frac{-ac^2+2bcd-ad^2}{a^2-b^2}\right]_{(r-1)},\\
d^{(r)}&=\left[\frac{-ad(c+c^*)+b(d^2+|c|^2)}{a^2-b^2}\right]_{(r-1)}.
\end{aligned} \tag{12}$$

The subscript $(r-1)$ means that quantities inside the parentheses should be taken at the given order of iteration. For the infinite ladder the behavior of the coefficients as a function of r is as follows. For $\phi<\phi_1$ and for l and γ below and up to the phase boundary the on-site coefficients a and b tend to constant values of opposite sign. On the phase boundary the absolute values are equal. For l and γ above the phase boundary they fluctuate around a constant value. This can be used to determine the phase boundary, in good numerical agreement with Ref. 2. The off-site coefficients c and d go to zero as a function of iteration. For $\phi>\phi_1$ the convergence of a and b towards constant values and that of c and d towards zero is slower than that for $\phi<\phi_1$. In fact, for this region it is the onset of oscillations which can be best used to determine the phase boundary.

For the surface problem we have the equations

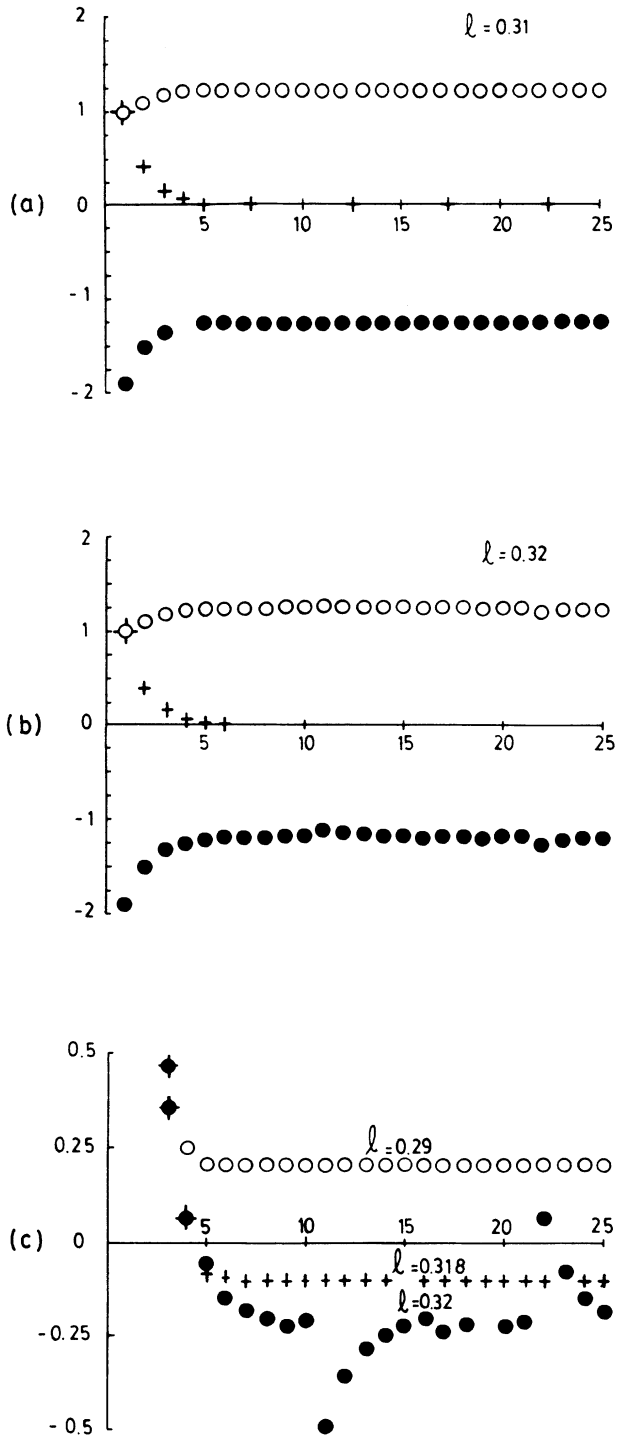

FIG. 2. Terminated ladder: (a) and (b) renormalized coefficients: a, solid circles; b, open circles; c, crosses as a function at the order of iteration for two different values of l. (a) For $l=0.31$, below the phase diagram of the infinite ladder; (b) for $l=0.32$, above the phase diagram. (c) Determinant (a^2-b^2) as a function of the order of iteration for different values of l: $l=0.29$ below the phase diagram (open circles); $l=0.318$ above the phase diagram of the terminated ladder but below that of the infinite ladder (crosses); $l=0.32$ above the phase diagram of the infinite ladder (solid circles).

$$\begin{aligned} &\underline{H}_s\underline{\psi}_0^{\dagger}\underline{U}^{\dagger}\underline{\psi}_1=\underline{0}\,, \\ &\underline{H}_0\underline{\psi}_n+\underline{U}\,\underline{\psi}_{n-1}+\underline{U}^{\dagger}\underline{\psi}_{n+1}=\underline{0}\,, \end{aligned} \tag{13}$$

where

$$\underline{H}_s=\begin{bmatrix} a_s & b_s \\ b_s & a_s \end{bmatrix}.$$

We can proceed as above eliminating every second node to the right of the surface, thus defining a renormalized semi-infinite ladder. After r steps of this procedure, the surface node is coupled to the node which originally was at site 2^r. It can be seen that at each iteration the coefficients are given by

$$a_s^{(r)}=a_s^{(r-1)}+\left[\frac{c_s(-ac^*+bd)+d_s(-db+c^*b)}{a^2-b^2}\right]_{(r-1)},$$

$$b_s^{(r)}=b_s^{(r-1)}+\left[\frac{c_s(-ad+cb)+d_s(bd-as)}{a^2-b^2}\right]_{(r-1)},$$

$$c_s^{(r)}=\left[\frac{c_s(bd-ac)+d_s(cb-ad)}{a^2-b^2}\right]_{(r-1)}.$$

Figure 2 shows the behavior of the coefficients as one proceeds with the iterations. It is seen that again in this case the connecting coefficients go to zero very rapidly for l and ϕ below and up to the phase boundary of the infinite ladder. Above this, they fluctuate but remain smaller than the on-site coefficients. The latter tend to constant values which are of equal magnitude and of opposite sign at the phase boundary for the semi-infinite ladder. These coefficients start to oscillate once we are above the phase boundary of the infinite ladder.

B. Impurity

The presence of one loop in the ladder of different size from the rest, i.e., an impurity, is of importance in systems that can be experimentally realized. For this reason we have considered the case in which the longitudinal strands joining nodes 0 and 1 have a length l' different from the rest. In such a case the equations for the Green functions read

$$\begin{aligned} &\underline{H}_1\underline{G}_{00}+\underline{B}^{\dagger}\underline{G}_{10}+\underline{U}\,\underline{G}_{-10}=\underline{1}\,, \\ &\underline{H}_1\underline{G}_{10}+\underline{U}^{\dagger}\underline{G}_{20}+\underline{B}\,\underline{G}_{00}=\underline{0}\,, \end{aligned} \tag{14}$$

where

$$\underline{H}_1=\begin{bmatrix} h & 1 \\ 1 & h \end{bmatrix},\quad \underline{B}=\begin{bmatrix} \beta & 0 \\ 0 & \beta^* \end{bmatrix},$$

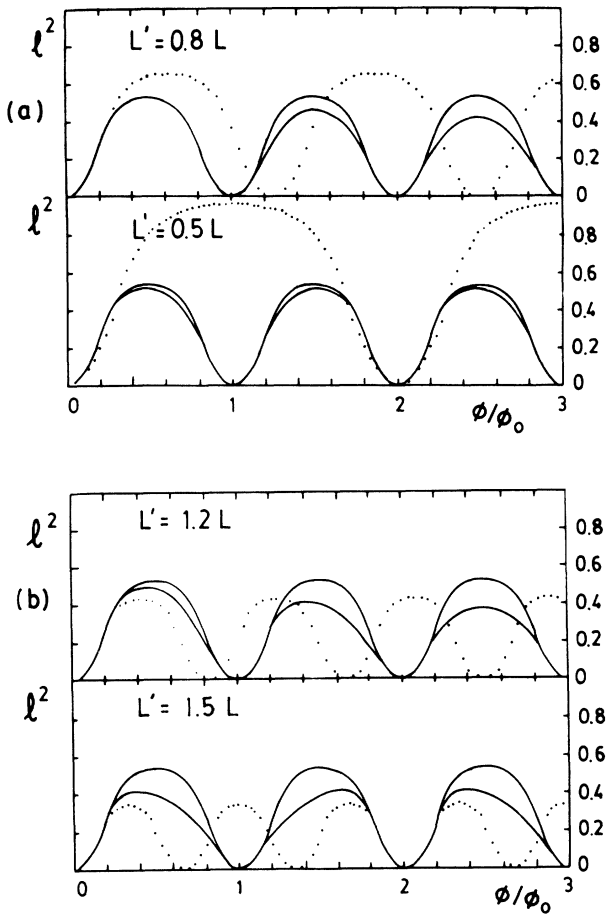

FIG. 3. Phase diagram for the impurity in the infinite ladder (lower solid line). Also shown is the phase diagram for the "pure-square" ladder (upper solid line) and for the "rectangular" ladder of the same dimensions as the impurity (dotted line). $L'=0.5L, 0.8L, 1.2L, 1.5L$. The phase boundary for the impure ladder is not periodic in ϕ/ϕ_0.

with $h=-3\cos l+\sin(l'-l)/\sin l'$ and $\beta=e^{i\gamma l'/l}\times\sin l/\sin l'$. With the use of the transfer matrix, Eqs. (14) can be solved to yield

$$(\underline{G}_{00})^{-1}=[\alpha\underline{1}-\underline{U}^{\dagger}\underline{T}_L^{-1}-\underline{B}^{\dagger}(\underline{1}-\underline{U}\,\underline{T}_R^{-1})^{-1}\underline{B}]\,, \quad (15)$$

where $\alpha=\sin(l'-l)/\sin l'$. Figure 3 shows the phase diagram for different l' values. Also shown is the phase diagram for a perfect rectangular ladder in which each loop is of the same dimensions as the impurity. The change in period on the flux axis is apparent. It is seen that for $\phi<\phi_1$, when superconductivity is uniform, the phase diagrams coincide. When a nonvanishing wave vector is dominant, the transition temperature of the smaller ladders goes down, because the deformation energy is distributed over a short length. The impurity is generally favored (higher transition temperature) when the magnetic flux is such that the fluxoid quantization condition is satisfied for the corresponding rectangular ladder. As a rule, the mode around the impurity is more extended when the corresponding transition temperature lies closer to the "pure" square case.

III. 2D SQUARE LATTICE AND SURFACE

The properties of a semi-infinite square lattice are of importance in the understanding of experimental results in these systems since a surface or border line will be a part of any real system. Before going into the surface problem we have looked at the perfect 2D square lattice, firstly, to check (in a nontrivial case) some of the methods we used against the solutions to this same problem obtained by other authors,[7] and secondly, to have a first-hand phase diagram to compare with the surface case.

The equivalent electron problem has recently been extensively discussed in the literature.[7-9] From the results obtained by Aubry it can be seen that the superconducting case coincides with the critical case of the electronic problem, corresponding to a value of the parameters where the states go from localized to extended. So for the superconducting case the states are probably localized with a power law, which poses problems for some of the methods that can be used. The nodal equations for the lattice read

$$-4(\cos l)\psi_{n,m}+e^{-in\gamma}\psi_{n,m}+e^{in\gamma}\psi_{n,m-1}+\psi_{n-1,m}+\psi_{n+1,m}=0. \quad (16)$$

If we look for solutions of the form $\psi_{n,m}=\psi_n e^{iqm}$, the above equations reduce to

$$\epsilon_n\psi_n-\psi_{n-1}-\psi_{n+1}=0\,, \quad (17)$$

where $\epsilon_n=4\cos l-\lambda\cos(q-n\gamma)$. For superconductivity, $\lambda=2$. By assuming that γ is of the form $\gamma=2\pi m/N$ where m/N is an irreducible fraction, the "energies" ϵ_n repeat after N steps in the chain represented by Eq. (17).

This introduces a periodicity in the system and defines a basis. We can exploit this translational invariance and reduce the problem of solving Eq. (16) for those particular γ values by diagonalizing the resulting $N\times N$ matrix. This procedure yields the phase diagram shown in Fig. 4. As pointed out by Hofstadter, the simplest fractions, such as $\frac{1}{2}$, $\frac{1}{3}$, etc., give rise to the dips which lend their special shape to this spectrum. The associated eigenstates are extended.

Another possibility is to apply a decimation tech-

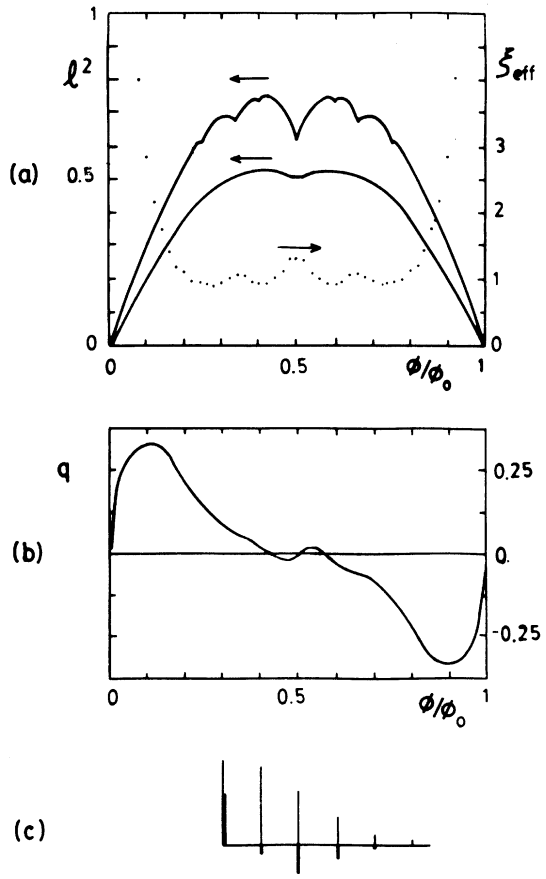

FIG. 4. Semi-infinite square lattice. (a) Phase diagram for the surface mode (lower solid line) and for the infinite square lattice (upper solid line). Note the dips for the simplest rational values of ϕ/ϕ_0. The dotted line is the effective coherence length for the surface mode, in units of L. The figure is periodic in ϕ/ϕ_0. (b) Transverse wave vector (q) (parallel to the surface) associated with the surface phase diagram. (c) Modulus of the order parameter (thin line) and currents (thick line) for the first branches parallel to the surface, for $\phi/\phi_0=\frac{2}{25}$.

nique within the basis of N sites, leaving a renormalized chain governed by the equations

$$(\epsilon_0 Q_{N-1}-P^R_{N-1}-P^L_{N-1})\psi^{(N)}_n-\psi^{(N)}_{n-1}-\psi^{(N)}_{n+1}=0\ , \tag{18}$$

where $\epsilon_0=4\cos l-2\cos q$, ϵ_n is as above, and $P_n=\epsilon_n P_{n-1}-P_{n-2}$; $Q_n=\epsilon_n Q_{n-1}-Q_{n-2}$ with $P_0=0$, $P_1=1$, $Q_0=1$, $Q_1=\epsilon_1$. Translational invariance allows us to write $\psi^{(N)}_n=\psi^{(N)}e^{ikn}$ so that the equation to be solved is

$$\epsilon_0 Q_{N-1}-P^R_{N-1}-P^L_{N-1}=2\cos k\ . \tag{19}$$

The phase boundary is associated with the largest eigenvalue, corresponding to $k=0$. In general, on the phase boundary there is degeneracy in q, i.e., there are several q values which are relevant at a given point on the phase boundary.

Together with these methods we have applied the RGD which is especially suitable for analyzing the cases where ϕ/ϕ_0 is irrational. To apply the method we rewrite Eq. (17) as

$$\epsilon^{(0)}_n\psi_n-t^{(0)}_{n+1}\psi_{n+1}-t^{(0)}_n\psi_{n-1}=0\ . \tag{20}$$

The recursion relations are

$$\epsilon^{(r)}_n=\left[\epsilon_n-\frac{t^2_n}{\epsilon_{n+1}}-\frac{t^2_{n-1}}{\epsilon_{n-1}}\right]_{(r-1)}\ ,$$
$$t^{(r)}_n=\left[\frac{t_n t_{n+1}}{\epsilon_{n+1}}\right]_{(r-1)}\ , \tag{21}$$

where the subscript $(r-1)$ has the same meaning as given previously.

This method provides a phase diagram which complements those previously obtained. For irrational ϕ/ϕ_0 the "band width," not shown in Fig 4, vanishes. Hofstadter had noted this tendency for increasing degree of commensurability. This can be taken as an indication of the localized character of the states. Because of the importance for the electronic problem we have checked the statement by Aubry that for $\lambda<2$ the states are extended, and that for $\lambda>2$ they are localized, where λ is the strength of the incommensurate potential. Within the RGD, one has that as a function of iteration the ratio $\epsilon^{(r)}_0/2t^{(r)}$ oscillates between $+1$ and -1 for extended states, whereas for localized states it goes to zero, as do both numerator and denominator. For the case of a surface or border line in the square lattice, the nodal equations for $n=0$ read

$$3(\cos l)\psi_{0,m}=\psi_{0,m+1}+\psi_{0,m-1}+\psi_{1,m}\ , \tag{22}$$

and for $n\geq 1$,

$$4(\cos l)\psi_{n,m}=e^{-in\gamma}\psi_{n,m+1}+e^{in\gamma}\psi_{n,m-1}+\psi_{n-1,m}+\psi_{n+1,m}\ . \tag{23}$$

Assuming a solution of the form $\psi_{nm}=\psi_n e^{iqn}$ we obtain

$$\epsilon_0\psi_0=\psi_1\ ,$$
$$\epsilon_n\psi_n=\psi_{n-1}+\psi_{n+1}\ , \tag{24}$$

where now $\epsilon_0=3\cos l-2\cos q$.

To solve this system we have used a continuous-fraction method, which is generated through the progressive elimination of the amplitude coupled to ψ_0. In the first step, this procedure eliminates ψ_1 and leaves ψ_0 coupled to ψ_2. In the next step we

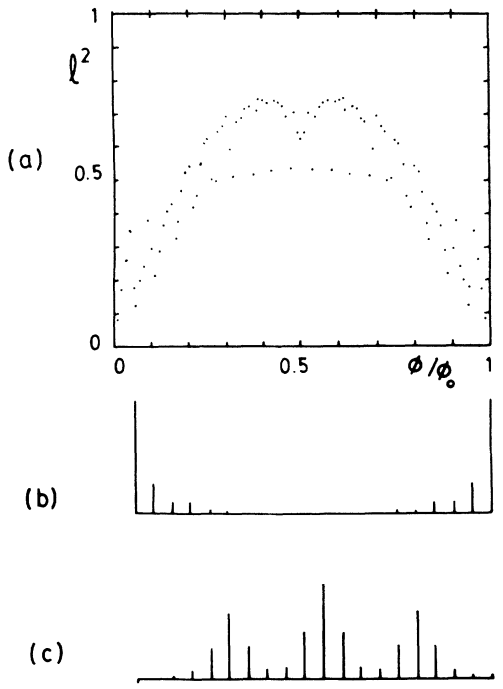

FIG. 5. Multiple ladder of $N=20$ longitudinal wires. (a) Phase diagram derived from the second eigenvalue, shown at discrete values of ϕ/ϕ_0, to allow for comparison with Fig. 4(a). The low-lying dots are degenerate with the phase boundary for the first eigenvalue. (b) Eigenvector associated with a degenerate eigenvalue at $\phi/\phi_0=\frac{37}{100}$. (c) Eigenvector associated with a nondegenerate eigenvalue at $\phi/\phi_0=\frac{1}{5}$.

eliminate ψ_2 and leave ψ_0 coupled to ψ_3, and so on. Carrying out this procedure until node n leads to the following relations:

$$\left[\epsilon_0-\frac{P_n}{Q_n}\right]\psi_0=\frac{1}{Q_n}\psi_{n+1}\,. \tag{25}$$

The coefficient $1/Q_n$ tends to zero very rapidly with n due to the localized nature of the surface state, and the phase boundary is obtained by finding the zeros of the left-hand coefficient in (25).

Figure 4(a) shows the phase boundary for the surface mode, compared with that of the infinite lattice. It can be seen that the surface nucleation appears at temperatures higher than the bulk transition temperature. Figure 4 also shows the effective coherence length with which the surface mode decays toward the inside of the lattice. From the initial slopes of both phase diagrams one can obtain the relation between H_{c3} and H_{c2} for this geometry, namely $H_{c3}=1.59\,H_{c2}$.

Figure 4(b) shows the q_m value associated with the phase-transition boundary for the surface. Associated with this mode there are currents flowing parallel to the surface, as for surface superconductivity. The net current is zero, as is for that case. There are some features of the present situation which are associated with fluxoid quantization. It can be seen from Fig. 4(b) that q_m and therefore the longitudinal currents change sign when ϕ/ϕ_0 goes through $\frac{1}{2}$. The wave vector q_m shows two other zeros corresponding to the smooth minimum in the phase-boundary line. From a study of the eigenvectors, it can be seen that this situation is associated with the fact that the order parameter has secondary maxima at the even-numbered branches towards the inside of the network. For $\phi/\phi_0=\frac{1}{2}$, the order parameter vanishes at the midpoint of the odd-numbered branches. Figure 4(c) shows the order parameter and the currents of this surface mode, for the first branches, at a given field value.

These properties are similar to those obtained in Ref. 2 for multiple ladders of N infinitely long wires joined by transverse strands. The first eigenvalue gives a phase diagram which for $N=20$ is already indistinguishable from that of Fig. 4(a) for the surface. The eigenvectors look very much like the one shown in Fig. 4(c). In Fig. 5 we show the phase diagram associated with the second eigenvalue for $N=20$. It can be seen that the points show a close resemblance to the bulk phase diagram for the square lattice. For small values of ϕ/ϕ_0 there is a large difference between both phase boundaries. This happens in the regions where the effective coherence length is large and both surfaces interfere. In addition, there are some values of ϕ/ϕ_0 where the points shown fall on the phase boundary for the first eigenvalue, i.e., there is degeneracy between these two eigenvalues. This corresponds to a removal of the degeneracy in q, the longitudinal wave vector. Corresponding by the associated eigenvector, as shown in Fig. 5(b), has the same value on both surfaces. Finally, Fig. 5(c) shows a typical eigenvector corresponding to the second eigenvalue in a case where there is no degeneracy.

ACKNOWLEDGMENTS

We acknowledge fruitful conversations with C. Balseiro, J. V. José, N. Majlis, and H. Pastawski. One of us (J.M.S.) acknowledges support from the Comisión Nacional de Energía Atómica. One of us (C.W.) acknowledges support from the Consejo Nacional de Investigaciones Científicas y Técnicas.

[1]P. G. de Gennes, C. R. Acad. Sci. Ser. II 292, 9 (1981); 292, 279 (1981); S. Alexander (unpublished); R. Rammal, T. C. Lubensky, and G. Toulouse, Phys. Rev. B 27, 2820 (1983).

[2]J. Simonin, D. Rodrigues, and A. López, Phys. Rev. Lett. 49, 944 (1982).

[3]H. J. Fink, A. López, and R. Maynard, Phys. Rev. B 26, 5237 (1982).

[4]R. F. Voss and R. A. Webb, Phys. Rev. B 25, 3446 (1982).

[5]J. M. Ziman, *Models of Disorder* (Cambridge University Press, Cambridge, 1979).

[6]J. B. Sokoloff and J. V. José, Phys. Rev. Lett. 49, 334 (1982).

[7]D. R. Hofstadter, Phys. Rev. B 14, 2239 (1976).

[8]S. Aubry, in *Bifurcation Phenomena in Mathematical Physics and Related Topics,* edited by C. Bardos and C. Bessis (Reidel, New York, 1920), pp. 163–184.

[9]C. M. Soukoulis and E. N. Economou, Phys. Rev. Lett. 48, 1043 (1982).